DOI: 10.1002/ejic.200500894

An Experimental and Density Functional Study of the Interaction of Cu^{II} Complexes of Diethylenetriamine (Dien) with Pyridine, Nicotinic Acid, and Nicotinamide: The Crystal Structure of [Cu(dien)(nicotinamide)$(NO_3)_2$]

Panagiotis A. Papanikolaou,[a] Panagiotis C. Christidis,[b] Aikaterini Th. Chaviara,[a] Christos A. Bolos,*[a] and Athanassios C. Tsipis*[c]

Keywords: Copper / Density functional calculations / N ligands / Thermal analysis

The reaction of pyridine (py), nicotinamide (nica), nicotinic acid (nic), and its nicotinate anion (nic^-) with [Cu(dien)X_2] (dien = diethylenetriamine; X = Br^-, NO_3^-) in a 1:1 molar ratio affords the new compounds [Cu(dien)(py)$(NO_3)_2$], [Cu(dien)(nica)$(NO_3)_2$], [Cu(dien)(nic^-)$(NO_3)(H_2O)$]·H_2O, [Cu(dien)(nic^-)(Br)(H_2O)]·$2H_2O$, and [Cu(dien)(NO_3)(nic^-)(Guo)]·$5H_2O$. These compounds were characterized by elemental analysis, and their molecular structures were determined by spectroscopic methods (infrared and electronic spectra), magnetic susceptibility, and molar conductivity measurements, and further corroborated by geometry optimization using electronic structure calculation methods at the B3LYP/6-31G(d,p) level of theory. The structural, bonding and electronic properties of the complexes are adequately described by B3LYP computational techniques. According to the experimental data, the complexes can be characterized in the solid state as mononuclear, with a distorted octahedral stereochemistry. The distorted octahedral stereochemistry adopted by the complexes was further confirmed by the X-ray structure analysis of [Cu(dien)(nica)$(NO_3)_2$], which consists of a six-coordinate Cu atom in a distorted octahedral environment constructed from four N atoms (three from dien and one from nica) and two O atoms from the loosely associated NO_3^- counteranions, with the former occupying the equatorial square plane of the octahedron and the latter the axial positions, Cu–O bond lengths being rather long (2.373 and 2.858 Å, respectively). Some substitution reactions have also been studied and are discussed in light of the electronic structure of the complexes computed at the B3LYP/6-31G(d,p) level.

Introduction

Nicotinamide (nica) and nicotinic acid (nic) are two of most extensively studied pyridine derivatives. The former is a component of the vitamin B complex and of the vital coenzyme NAD (nicotinamide adenine dinucleotide),[1] and is a typical N-donor ligand system in crystal engineering.[2] Furthermore, early administration of nicotinamide has been reported to impair learning and memory in mice.[3] The medicinal chemistry of nicotinamide in the treatment of ischemia and reperfusion has also developed rapidly in the past few years. Nicotinic acid has a wide-ranging ability to reduce lipid levels, but its clinical uses are restricted due to its various side-effects. Nicotinic acid and nicotinamide form niacin, a water-soluble vitamin that reduces VLDL cholesterol and increases HDL cholesterol (the so-called "good" cholesterol).[4] Moreover, coordination compounds of nicotinic acid, nicotinamide, and their derivatives are known to have antiviral or antibacterial activity,[5,6] and they also selectively affect tumor tissues.[7]

Preliminary toxicity and anticancer results of diethylenetriamine (dien)–Cu^{II} mixed-ligand complexes with nicotinic acid (nic) and nicotinamide (nica) ligands encouraged us to thoroughly study such complexes. In effect, what we want to address here is the synthesis and the structural, bonding, electronic, and spectroscopic properties of a number of new compounds resulting from interaction of [Cu(dien)X_2] (X = Br^-, NO_3^-) with pyridine (py), nicotinic acid, and nicotinamide. The electronic structure and bonding of the new complexes was inferred from electronic structure calculation methods at the DFT level.

Results and Discussion

Synthesis

The synthetic procedures used to prepare the new complexes can be divided into two categories: the first method is based on the reaction of [Cu(dien)$(NO_3)_2$] with nicotinic acid (nic), nicotinamide (nica), or pyridine (py), while the second one involves the reaction of deprotonated nic (nic^-)

[a] Laboratory of Inorganic Chemistry, Department of Chemistry, Aristotle University of Thessaloniki, 54124 Thessaloniki, Greece
[b] Laboratory of Crystallography, Department of Physics, Aristotle University of Thessaloniki, 54124 Thessaloniki, Greece
[c] Section of Inorganic and Analytical Chemistry, Department of Chemistry, University of Ioannina, 451 10 Ioannina, Greece
E-mail: attsipis@cc.uoi.gr

with [Cu(dien)$(NO_3)_2$] (**1**) or [Cu(dien)Br_2] (**2**). Both syntheses were performed in methanol using a 1:1 molar ratio of the reactants. The new Cu^{II} complexes, formulated as [Cu(dien)(py)$(NO_3)_2$] (**3**), [Cu(dien)(nica)$(NO_3)_2$] (**4**), [Cu(dien)(nic^-)$(NO_3)(H_2O)$]·H_2O (**5**), [Cu(dien)(nic^-)(Br)-(H_2O)]·$2H_2O$ (**6**), and [Cu(dien)(NO_3)(nic^-)(Guo)]·$5H_2O$ (**7**), are paramagnetic, as expected from the d^9 electron configuration of the Cu^{II} central atom, blue in color, and stable in air. They are soluble in water and other coordinating solvents such as DMF and DMSO, slightly soluble in alcohols, but insoluble in common organic solvents.

Spectroscopy

The salient structural features of the new complexes were determined by spectroscopic methods (infrared and electronic spectra), while details of the structures were obtained by the X-ray structural investigation of a representative complex, namely [Cu(dien)(nica)$(NO_3)_2$] (**4**). In the IR spectra of the precursor complexes [Cu(dien)$(NO_3)_2$] (**1**) and [Cu(dien)Br_2] (**2**) the absorption bands at around 3270 and 3233 cm^{-1} are attributed to the antisymmetric and symmetric stretching vibration of the primary and secondary amino group of dien, respectively, thus confirming the tridentate coordination bonding mode of the ligand.[9] In the IR spectrum of [Cu(dien)(py)$(NO_3)_2$] (**3**), the ν(C=N) stretching vibration at 1608 cm^{-1} is shifted towards lower frequencies with respect to that of the free pyridine (1622 cm^{-1}), thereby indicating coordination of the pyridine through the endocyclic nitrogen atom. The same also holds true for the rest of the complexes involving the nic and nic^- ligands. In contrast, upon coordination of the nica ligand the absorption band at 1593 cm^{-1} is shifted slightly towards higher frequencies (1603 cm^{-1}), in line with previous observations.[10] The new bands at around 520–535 cm^{-1} due to ν(Cu–N) stretching vibrations[11] confirm the N-coordination of py and its derivatives through the endocyclic nitrogen atom. In addition, the experimental ν(C=O) stretching vibration of the free nicotinamide ligand appearing at 1681 cm^{-1} is slightly shifted to higher frequencies (1693 cm^{-1}) upon coordination to the metal center in [Cu(dien)(nica)$(NO_3)_2$] (**4**), in line with previous studies.[12–14] In the IR spectrum of nicotinic acid the ν(C=O) stretching vibration absorbing at 1709 cm^{-1}[15,16] is shifted to lower frequencies (1661–1668 cm^{-1}) upon coordination, regardless of the deprotonation of the ligand. Moreover, the IR spectra of [Cu(dien)-(NO_3)(nic^-)]·$2H_2O$ (**5**) [Cu(dien)(Br)(nic^-)]·$3H_2O$ (**6**), and [Cu(dien)(NO_3)(nic^-)(Guo)]·$5H_2O$ (**7**) show that the nic^- ligand is not coordinated through the N atom of the pyridine ring. The two IR absorption bands at 1760 and 1745 cm^{-1}, combined with a very intense and broad band at around 1380 cm^{-1}, are indicative of the unidentate coordination mode of the nitrate anions with copper(II). Finally, the very weak band at 324 cm^{-1} should be attributed to the ν(Cu–Br) stretching vibration of **6**.[11] The presence of water in all hydrated complexes, either as ligands or as lattice water, as well as the large number of hydrogen bonds, was indicated by the appearance of broad bands at 3414 and 3476 cm^{-1}, respectively. The former can be attributed to hydrogen bonds and the latter to the existence of water either in the lattice or as a ligand. The presence of water was further corroborated by thermal DTA analysis (vide infra).

The UV/Vis electronic spectra of the complexes in aqueous 10^{-3} M solutions show a band in the visible region at 608–623 nm (Figure 1), which can be attributed to crystal-field d–d electronic transitions (probably $3d_{x^2-y^2} \leftarrow 3d_{z^2}$). This band is characteristic for Cu^{II} complexes with a distorted square-pyramidal geometry.

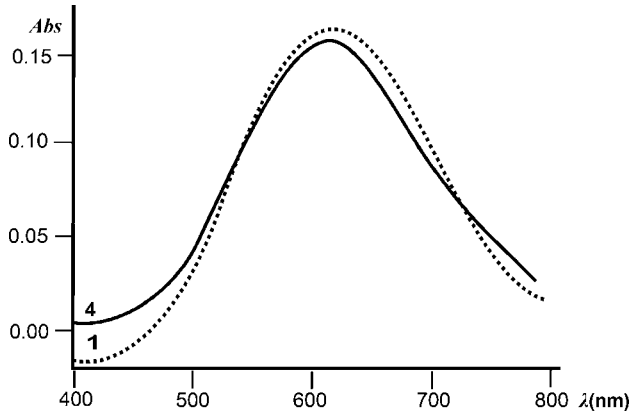

Figure 1. Electronic spectra of [Cu(dien)$(NO_3)_2$] (**1**) and [Cu(dien)-(nica)$(NO_3)_2$] (**4**) in aqueous solution.

In the UV region of the spectra of the "free" py, nic, nic^-, and nica ligands the absorption bands and shoulders occur around 240–260 nm ($\log\varepsilon$ = 3.63–3.90), which can be attributed to intraligand π* ← π electronic transitions due to the conjugated C=N, C=C, and C=O groups of the pyridine-ring-containing ligands. These bands are shifted either to lower or higher frequencies, depending on the coordination mode of the ligand. The band at 204–214 nm could be assigned to σ* ← σ type transitions of the free dien molecule, which is not shifted upon coordination.

In the solid state (Nujol mulls), all Cu^{II} complexes show the crystal-field band at around 560–580 nm. Such bands are typical for octahedral Cu^{II} complexes. Therefore, it is obvious that the different structures adopted by the complexes in aqueous and methanol solutions and in the solid state may be due to the dissociation of the compounds in solution.[17]

Conductivity and Magnetic Measurements

The molar conductivity values, Λ_μ, for the complexes, which vary between 159–423 and 77–213 μS cm^{-1} for 10^{-3} M aqueous and methanol solutions, respectively, strongly suggest the ionic nature of the complexes. Specifically, in aqueous solutions, the zwitterionic complexes [Cu(dien)(nic^-)-$(NO_3)(H_2O)$]·H_2O (**5**), [Cu(dien)(nic^-)(Br)(H_2O)]·$2H_2O$ (**6**), and [Cu(dien)(NO_3)(nic^-)(Guo)]·$5H_2O$ (**7**) are 1:1 electrolytes[18] that dissociate according to the following general scheme:

$[Cu(dien)(X)(nic^-)(H_2O)] \rightleftharpoons [Cu(dien)(nic^-)]^+ + X^-$ (X = NO_3^-, Br^-)

$[Cu(dien)(py)(NO_3)_2]$ (**3**) and $[Cu(dien)(nica)(NO_3)_2]$ (**4**) are 2:1 electrolytes in aqueous solutions, with two dissociating nitrate anions. In methanol solution, complexes **3**–**7** are 1:1 electrolytes. Taken together, the above data lead to the conclusion that the complexes dissociate to a lesser degree in methanol solution.

The μ_{eff} values for the Cu^{II} complexes were found in the range 1.72–1.93 μ_B, consistent with their mononuclear structures.

Thermal Analysis

The thermal behavior of selected Cu^{II} complexes was studied by TG/DTG/DTA thermal analysis in the temperature range 40–1000 °C. The intermediates were confirmed from the mass-loss calculations. Generally, the thermal decomposition of the complexes proceeds in 4–6 stages, which depend on the nature of the ligands involved. For example, the thermal behavior of **4** (Figure 2) is characterized by four decomposition stages. The first one (200–281 °C) corresponds to the removal of the dien and nica ligands, while during the next two stages, which are non-distinct (281–519 and 519–865 °C), the successive decomposition of two nitrate ions to a nitrite moiety takes place; the calculated and found values for this process are almost identical. During the fourth step (865–973 °C), the elimination of an oxygen molecule, derived from the decomposition of two nitrate ions to the corresponding nitrito moiety, occurs. The elimination of O_2 at such a high temperature should be due to its strong binding with Cu as a CuO_2 fragment. The last step corresponds to the formation of metallic copper as a residue, as proved by IR spectroscopy and its quantitative analysis.

The thermal analysis of **5** (Figure 3) starts with the dehydration of the molecule, which takes place in a single mass-loss step corresponding to 9.2% (calcd. 9.3%), up to 123 °C, due to the endothermic elimination of lattice and coordinated water molecules. A total weight loss of 58.00% occurs in the temperature range 212–327 °C, presumably due to the loss of nic^- and dien ligands (calcd. 58.22%). The third step (665–964 °C) involves loss of the nitrate anion, while the residue remaining at temperatures higher than 964 °C is metallic copper, as evidenced by the mass loss (calcd. 16.45; found 16.80%) and the IR spectroscopic data.

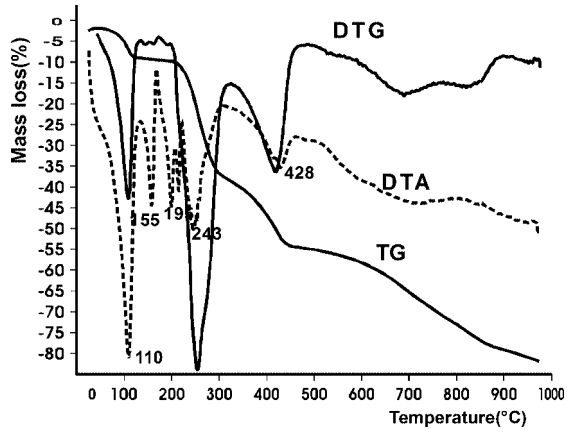

Figure 3. Thermal analysis diagram of $[Cu(dien)(nic^-)(NO_3)(H_2O)]\cdot H_2O$ (**5**).

Complex **6** partly dehydrates up to 110 °C in a single mass-loss process that corresponds to the endothermic elimination of two lattice water molecules, for which the theoretical and experimental mass loss are almost the same (Figure 4). The removal of the nicotinate anion takes place in the temperature range 216–300 °C in a second endothermic mass-loss procedure (28.75% found, 29.36% theoretical), as was proposed by Yeh et al.[19] The Br atom is removed between 300 and 432 °C (18.75% found, 19.37% calcd.), while the liberation of the dien molecule takes place at 432–848 °C (24.38% found, 24.97% calcd.). The elimi-

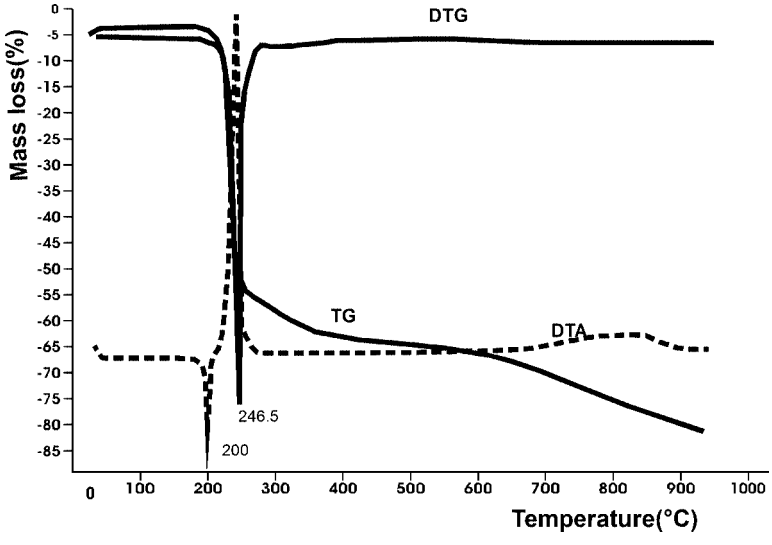

Figure 2. Thermal analysis diagram of $[Cu(dien)(nica)(NO_3)_2]$ (**4**).

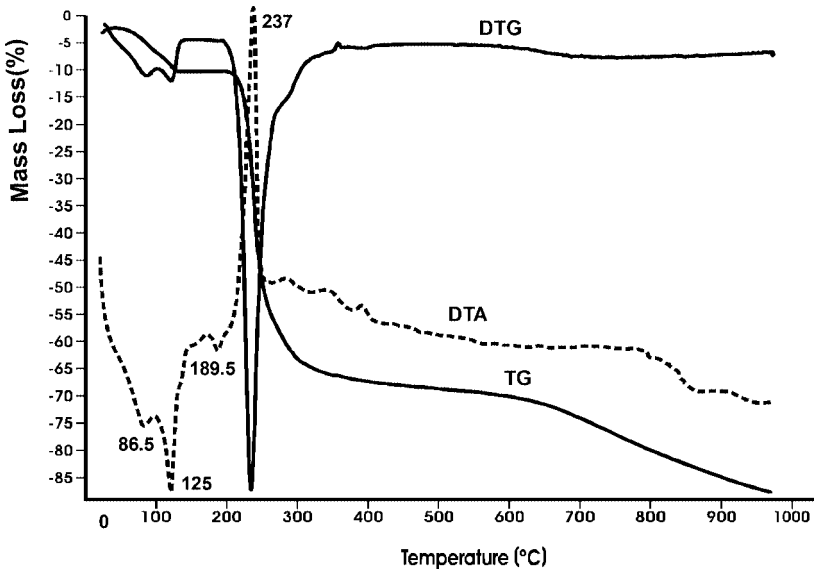

Figure 4. Thermal analysis diagram of [Cu(dien)(nic$^-$)(Br)(H_2O)]·2H_2O (**6**).

nation of the coordinated water at a higher temperature (848–964 °C) is tentatively proposed. The solid residue of the procedure above 964 °C corresponds to metallic copper.

Crystal Structure of [Cu(dien)(nica)(NO_3)$_2$] (4)

The molecular structure of **4** is shown in Figure 5, while bond lengths and angles along with the established hydrogen bonds are given in Table 1. The coordination polyhedron around the Cu^{II} central atom is a distorted octahedron (4 + 1 + 1) with three of the equatorial positions occupied by the three nitrogen atoms of the dien ligand and the fourth position occupied by the nitrogen atom of the pyridine ring. The two axial positions of the coordination polyhedron are occupied by oxygen atoms from each of the two NO_3^- anions at considerably different distances from the copper atom [Cu1–O2 = 2.373(2) and Cu1–O5 = 2.858(3) Å]. The conformation of the dien ligand is as expected.[21–23] The Cu–N distances range from 1.998(3) to 2.015(3) Å, while both the N^p–Cu–N^s valence angles (N^p from primary and N^s from secondary amino groups) are smaller than 90° [84.1(1)° and 84.3(1)°]. Moreover, the N^p–Cu–N^p angle is much smaller than 180° [163.7(1)°], which indicates a slight strain in the coordinated dien ligand. The reported observation that the Cu–N^s distance is significantly shorter than the Cu–N^p distances[22,24] seems to be generally valid only when referred to the mean Cu–N^p distance [compare, for example, the Cu–N(dien) distances reported previously[8,25]]. The Cu–N(pyridine) distance of 2.036(3) Å deviates only slightly from the mean Cu–N(dien) distance [2.005(5) Å]. The four equatorial nitrogen atoms of the copper coordination polyhedron lie almost on a plane (rms deviation of the fitted atoms of 0.06 Å), forming an angle of 58.9(1)° to the plane of the pyridine ring. The copper atom deviates significantly from the above equatorial plane by 0.150(2) Å towards the axial O(2) atom with the shorter Cu–O bond. The established geometry of the pyridine ring is as expected, with the C–C bond lengths lying in the range 1.375(5)–1.391(5) Å and the C–N bond lengths lying in the range 1.333(4)–1.339(4) Å. The two nitrato groups also have a normal geometry, with the N6–O and N7–O bond lengths ranging from 1.226(4) to 1.258(4) Å and 1.217(4) to 1.246(4) Å, respectively.

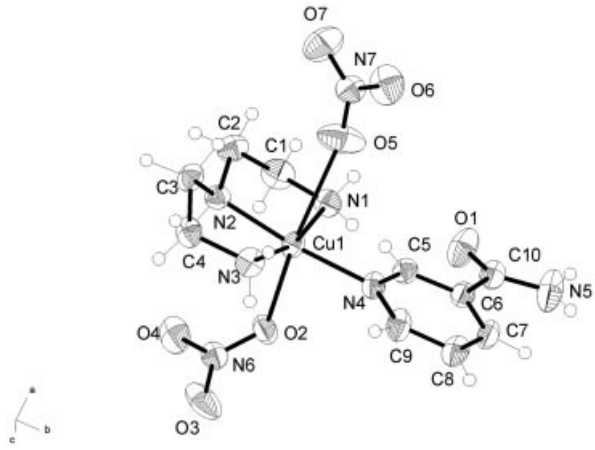

Figure 5. DIAMOND[20] plot of the molecular structure of [Cu(dien)(nica)(NO_3)$_2$] (**4**), with the labeling scheme of the non-H atoms. Displacement ellipsoids are shown at the 30% probability level.

Hydrogen bonding plays a predominant role in the stabilization of the structure. As can be seen from Table 1, both the N^p atoms of the dien ligand and the N atom of the amide group donate exclusively to oxygen atoms of NO_3 groups of neighboring molecules, while the N^s atom of the dien ligand donates to the oxygen atom of the amide group of another molecule.

Table 1. Selected bond lengths [Å] and angles [°] for [Cu(dien)(nica)$(NO_3)_2$] (**4**).

Cu1–N1	2.015(3)	C2–N2	1.476(5)
Cu1–N2	2.002(3)	C3–N2	1.479(5)
Cu1–N3	1.998(3)	C3–C4	1.499(6)
Cu1–N4	2.036(3)	C4–N3	1.482(5)
Cu1–O2	2.373(2)	C6–C10	1.515(5)
Cu1–O5	2.858(3)	C10–N5	1.321(5)
C1–N1	1.479(5)	C10–O1	1.211(4)
C1–C2	1.503(6)		
N1–Cu1–N2	84.11(13)	C3–C4–N3	109.0(3)
N2 –Cu1–N3	84.31(13)	Cu1–N4–C5	122.5(2)
N3–Cu1–N4	97.30(13)	Cu1–N4–C9	119.4(2)
N1–Cu1–N4	93.20(13)	C5–N4–C9	117.8(3)
N1–C1–C2	107.9(3)	C6–C10–N5	117.6(3)
C1–C2–N2	107.8(3)	C6–C10–O1	119.9(3)
C2–N2–C3	116.8(3)	N5–C10–O1	122.4(4)
N2–C3–C4	107.6(3)		

Hydrogen bonding geometry

D–H···A	D–H [Å]	H···A [Å]	D···A [Å]	D–H···A [°]
N1–H9A···O5[a]	0.86(4)	2.50(4)	3.167(5)	135(3)
N1–H9A···O7[a]	0.86(4)	2.54(4)	3.290(4)	146(3)
N1–H9B···O6	0.87(4)	2.40(4)	3.216(4)	157(3)
N2–H10···O4	0.88(4)	2.44(4)	3.161(5)	140(3)
N2–H10···O1[a]	0.88(4)	2.42(4)	3.064(4)	131(3)
N3–H11A···O2[b]	0.71(4)	2.57(4)	3.261(4)	168(4)
N3–H11A···O3[b]	0.71(4)	2.45(4)	2.940(5)	128(4)
N3–H11B···O6[c]	0.85(5)	2.34(5)	3.178(5)	166(4)
N5–H12A···O6[d]	0.79(5)	2.19(5)	2.967(5)	167(5)
N5–H12B···O7[e]	0.94(5)	2.16(5)	3.079(5)	168(4)

[a] Symmetry codes: x, 1/2 – y, 1/2 + z. [b] x, 1/2 – y, –1/2 + z. [c] –1 + x, y, z. [d] 1 – x, –y, –z. [e] 1 – x, –1/2 + y, –1/2 – z.

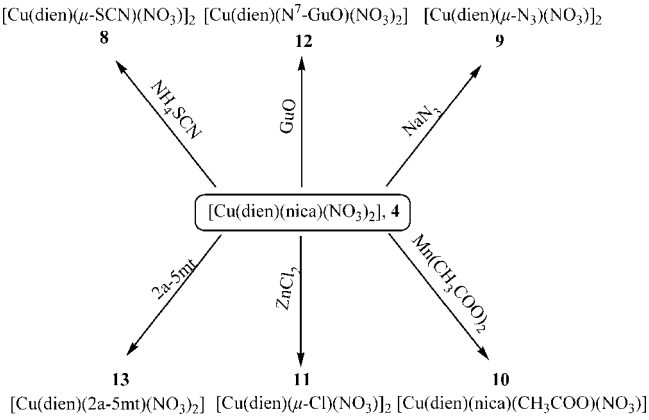

Scheme 1. Reactivity of [Cu(dien)(nica)$(NO_3)_2$] (**4**) towards nucleophiles.

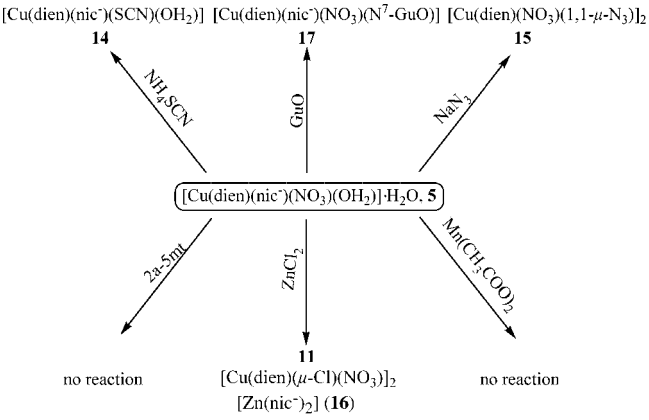

Scheme 2. Reactivity of complex **5** towards nucleophiles.

Reactivity of [Cu(dien)(nica)$(NO_3)_2$] (4) and [Cu(dien)(NO_3)(nic$^-$)(OH_2)]·H_2O (5)

We selected [Cu(dien)(nica)$(NO_3)_2$] and the zwitterionic complex [Cu(dien)(NO_3)(nic$^-$)(OH_2)]·$2H_2O$ to exploit their chemical reactivity towards nucleophiles. In particular, the zwitterionic form is expected to exhibit interesting reactivity due to the different electronic, steric, and nucleophilicity factors of the coordinated dien, NO_3, H_2O, nic$^-$, and nica ligands. The reactivity studies were performed using the reaction of a water/methanol solution of the precursor complex with various nucleophiles, such as SCN^-, N_3^-, Cl^-, CH_3COO^-, guanosine (GuO), and 2-amino-5-methylthiazole (2a-5mt) in a 1:1 molar ratio. All the reactions of complexes **4** and **5** studied are depicted schematically in Schemes 1 and 2, respectively.

The reaction products were identified by elemental analysis, spectroscopic measurements (IR and UV/Vis spectra), and magnetic and molar conductivity measurements, and the results compared with the experimental data available.[26] All reaction products are blue crystalline solids that are very soluble in water and in coordinating solvents, and slightly soluble in alcohols. The compounds are monomers or dimers and their magnetic moments are as expected for the d^9 electron configuration of Cu^{II}.

The reaction of **4** with NH_4SCN or NaN_3 leads to the nucleophilic substitution of the nica and one of the NO_3^- ligands to afford the dinuclear complexes [Cu(dien)(μ-SCN)$(NO_3)_2$] (**8**) and [Cu(dien)(μ-N_3)$(NO_3)_2$] (**9**), which are bridged by the ambidentate SCN^- and N_3^- ligands, respectively. In the IR spectra of **8** and **9** the bands related with the nicotinamide ligand disappear, while the new bands absorbing at 2073 and 2049 cm^{-1} are characteristic of the coordinated thiocyanate and azide ligands, respectively. The dinuclear nature of **8** and **9** was further confirmed by their molar conductivity values of 240–250 μS cm^{-1} in water solutions, which are indicative of the 1:2 electrolytic character of the complexes due to the dissociation of the NO_3^- counterion. The UV/Vis spectroscopic data of **8** and **9** in the solid state are characteristic of Cu^{II} complexes with octahedral stereochemistry.[26]

The reaction of **4** with $Mn(CH_3COO)_2·4H_2O$ leads to the substitution of one nitrate ion by an acetato group to yield [Cu(dien)(nica)$(CH_3COO)(NO_3)$] (**10**). This was confirmed by the IR spectrum of **10**, where the nitrato peak at 1749 cm^{-1} has disappeared and a new band at 1604 cm^{-1}, characteristic of the acetate ligand, has appeared. The acetate ligand binds in a κO fashion.[27]

The analytical and spectroscopic data of the crystals isolated from the reaction mixture resulting from the reaction of **4** with $ZnCl_2$ correspond to the dinuclear Cu^{II} complex formulated as [Cu(dien)(μ-Cl)]$_2$·[NO_3]$_2$ (**11**), which contains

bridging chloride ligands.[28] The reaction of **4** with Guo or 2a-5mt leads to the formation of the adducts [Cu(dien)(N^7-Guo)(NO_3)$_2$] (**12**) and [Cu(dien)(2a-5mt)(NO_3)$_2$] (**13**) by replacement of the coordinated nica ligand with the respective nucleophile. The IR spectra of **12** and **13** show the presence of characteristic bands for guanosine and 2-amino-5-methylthiazole, which are indicative of their coordination with copper(II), while the UV/Vis spectra suggest an octahedral geometry of the complexes. The molecular structure of **12** has been determined previously by X-ray crystallography.[29]

The reaction of the zwitterionic complex **5** with NH_4SCN yields blue needles of the mixed-ligand complex [Cu(dien)(NCS)(nic^-)(H_2O)] (**14**) by substitution of the nitrate ion by the thiocyanato ligand. The substitution reaction was monitored by the disappearance of the two bands at 1745 and 1380 cm^{-1} due to the stretching vibration of the nitrato ligands, and the appearance of the strong and sharp band at 2072 cm^{-1} due to the isothiocyanato ligand coordinated as a terminal ligand through its hard N-end.[30] The bands due to nic^- remain almost unchanged.

The reaction of **5** with NaN_3 leads to the replacement of both the nic^- ligand and the coordinated H_2O molecule by the azido ligand, which bridges the two Cu^{II} centers in an asymmetric end-on fashion to afford the dinuclear complex [Cu(dien)(NO_3)(1,1-μ-N_3)]$_2$ (**15**). The end-on bridging mode of the N_3^- group was proved by the presence of one intense band at 2049 cm^{-1}.

The reaction of **5** with $ZnCl_2$ leads to the dissociation of the complex and the formation of two new complexes: one of them, which is blue, corresponds to the dinuclear complex **11**.[28] Specifically, the IR spectrum of **11** is dominated by the absence of peaks for the nic^- ligand, while the bands at 344 and 388 cm^{-1} confirm the bridging mode of the chloro ligand. Moreover, the molar conductivity value (238 μS cm^{-1}) in water substantiates the 1:2 electrolytic nature of **11**. The second complex is a white solid that corresponds to Zn(nicotinate)$_2$ (**16**), where the Zn center is coordinated by two bidentate chelating carboxylato groups of the nicotinate anions.

Finally, the reaction of **5** with guanosine leads to the formation of the adduct [Cu(dien)(nic^-)(NO_3)(N^7-Guo)] (**17**) by replacement of the coordinated H_2O ligand. The IR spectrum of **17** shows the presence of both nic^- and Guo bands, which are indicative of their coordination with the copper(II) center, while the UV/Vis spectra suggest an octahedral stereochemistry for the CuN_5O chromophore. The reactions of complexes **4** and **5** with guanosine clearly mirror their ability to react with DNA components in the cell nucleus, which, in turn, could open up a new pathway for their further biological studies. Despite many attempts, the reactions of **5** with Mn($OOCCH_3$)$_2$·4H_2O or 2-amino-5-methylthiazole were unsuccessful.

Computational Studies Using DFT

Equilibrium Geometries, Electronic Structure, and Bonding Mechanism of [Cu(dien)(nic)] and [Cu(dien)(nica)] Complexes

In an attempt to understand some marked structural features of the complexes under investigation, we performed electronic-structure calculations based on density functional theory at the B3LYP/6-31G(d,p) level. We started the calculations with the various possible forms of nicotinic acid that exist in aqueous solutions. These species, along with their pK values,[31] are shown in Scheme 3.

The equilibrium geometries of the various forms of nicotinic acid (**A**, **B**, and **C**) and that of a deprotonated form of **A** at the heterocyclic N-atom (**A′**), computed at the B3LYP/6-31G(d,p) level, are given in Figure 6. No significant structural differences can be observed in the pyridine ring of the various forms of nicotinic acid. However, there are some changes in the structural parameters of the carboxylic group. For instance, the C–COO^- bond lengthens and the OCO bond angle decreases upon going from **B** to **C**, following the trend **B** > **A** > **A′** > **C**.

The vibrational frequencies obtained from our calculations are in line with those obtained from a previous theoretical study by Sala et al.[32] The β(COO) in-plane pyridinic ring deformation appears at 629, 631, and 625 cm^{-1} for **A′**, **B**, and **C**, respectively, and the ν(C=O) stretching vibration appears at 1855 and 1796 cm^{-1} for **A′** and **B**, respectively.

The various forms of nicotinic acid are expected to act as ambidentate ligands that coordinate to a metal center either through the carboxylato O- or heterocyclic N-donor atoms. This is clearly illustrated by their frontier molecular orbitals (FMOs; Figure 7).

In both **A** and **A′** the two occupied FMOs (HOMO and HOMO–1), which are involved in the formation of a coor-

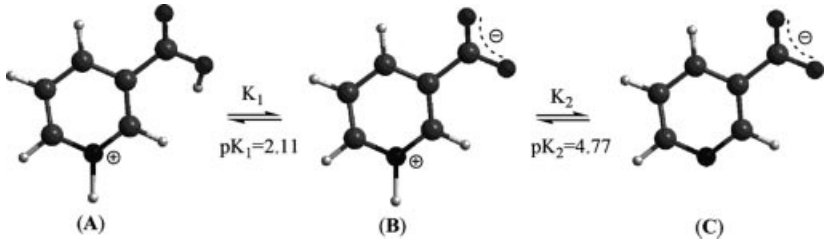

Scheme 3.

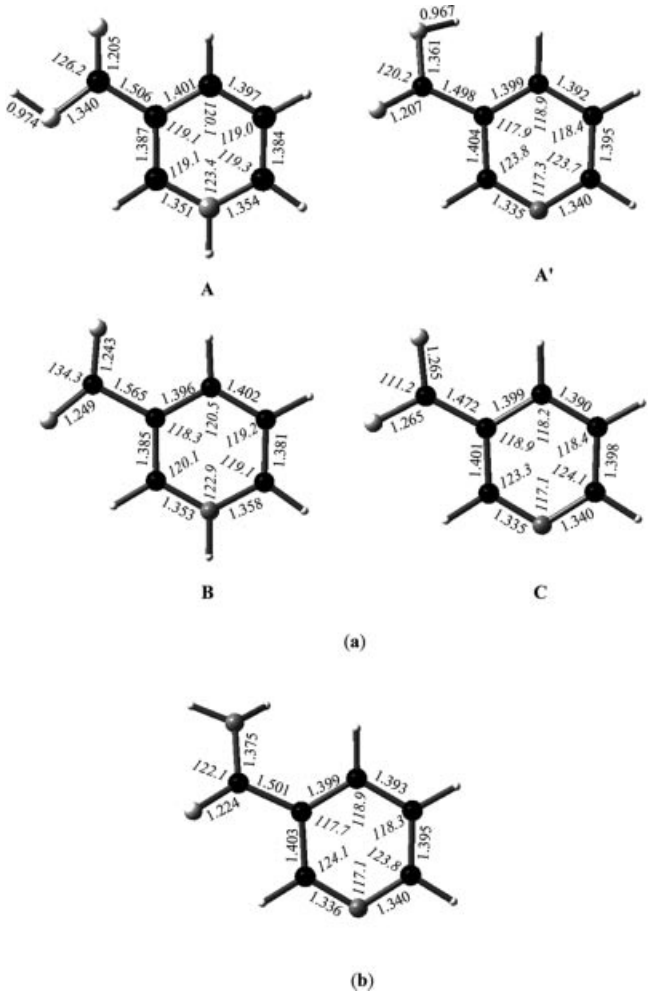

Figure 6. Equilibrium geometries of the various forms of nicotinic acid that exist in aqueous solution (a) and nicotinamide (b) computed at the B3LYP/6-31G(d,p) level of theory.

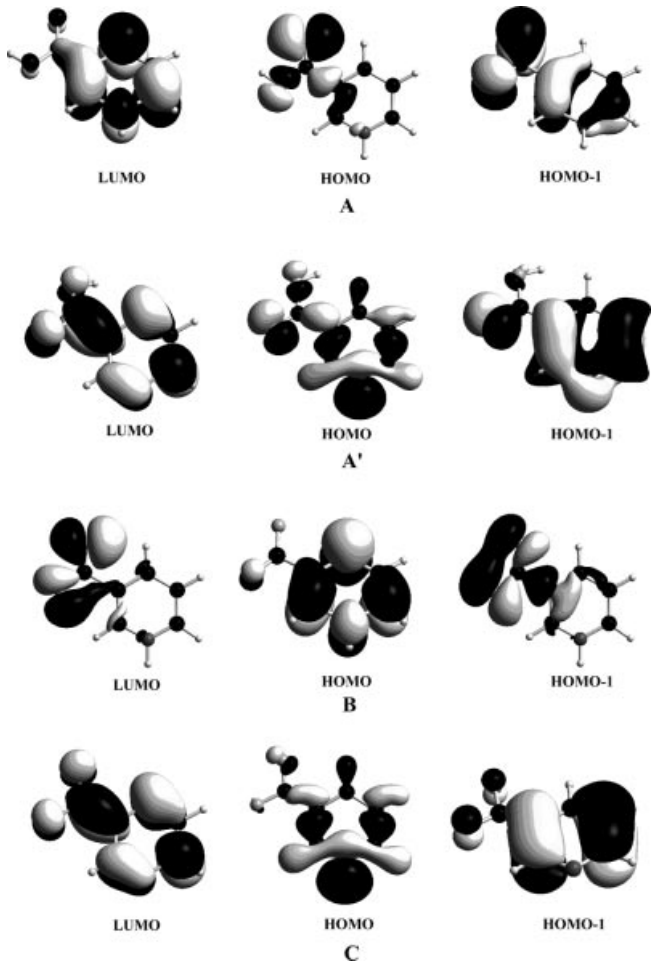

Figure 7. Frontier molecular orbitals (FMOs) of the various forms of nicotinic acid calculated at the B3LYP/6-31G(d,p) level.

dination bond with the Cu^{II} central atom, have significant contributions from p-AOs of the carboxylato O-donor atoms. However, the HOMO–1 has a significant contribution from a p-AO of the heterocyclic N-donor atom only in **A′**. In the latter, the unoccupied FMO (LUMO) has significant contributions from p-AOs located on the carboxylato O- or heterocyclic N-donor atoms, which could be involved in a π-back-bonding interaction with the central

Table 2. Selected energetic and electronic properties along with proton affinities (PA) of the various forms of nicotinic acid and nicotinamide calculated at the B3LYP/6-31G(d,p) level.

Property	**A**	**A′**	**B**	**C**	nica
E [hartrees]	–437.118717	–436.751872	–436.711249	–436.100562	–416.882167
E_{homo}	–0.44047	–0.26242	–0.19291	–0.27399	–0.25179
E_{lumo}	–0.26295	–0.06366	–0.10234	–0.07168	–0.05065
Q(N)[a]	–0.48	–0.44	–0.49	–0.43	–0.45
Q(O)	–0.54	–0.6	–0.7	–0.34	–0.6
Q(OH)	–0.71	–0.66	–0.72	–0.43	
nec(N)[a]	$2s^{1.25}2p^{4.22}$	$2s^{1.40}2p^{4.02}$	$2s^{1.25}2p^{4.22}$	$2s^{1.40}2p^{4.0}$	$2s^{1.38}2p^{4.05}$
nec(O)	$2s^{1.70}2p^{4.81}$	$2s^{1.73}2p^{4.85}$	$2s^{1.73}2p^{4.96}$	$2s^{1.74}2p^{4.67}$	$2s^{1.70}2p^{4.89}$
nec(OH)	$2s^{1.68}2p^{5.02}$	$2s^{1.64}2p^{5.00}$	$2s^{1.73}2p^{4.96}$	$2s^{1.75}2p^{4.59}$	
bop(C–COO)[b]	0.28	0.27	0.13	0.26	0.26
bop(C=O)	0.58	0.55	0.5	0.42	0.61
bop(C–OH)[c]	0.29	0.27	0.51	0.37	0.26
η [eV]	4.83	5.41	2.46	5.5	5.47
μ_e [D]	6.8	5.5	13.8	3.3	4.9
PA(N) [kcal mol^{-1}]	230.2	230.2	383.2	383.2	225.8
PA(O) [kcal mol^{-1}]	255.7	255.7	408.7	408.7	213.2

[a] Natural charges. [b] Mulliken bond overlap populations [for nica it refers to the C–CO(NH$_2$) bond]. [c] C–NH$_2$ for nica.

Cu^{II} atom. The HOMO and LUMO eigenvalues, along with selected electronic properties of the various nicotinic acid forms, are compiled in Table 2.

The proton affinities (PA) of the various forms of nicotinic acid calculated at the B3LYP/6-31G(d,p) level are also given in Table 2. Based upon the PA values, it is expected that the σ-donor ability of **C** and **B** through either the N- or O-donor atoms should be higher than that of **A** or **A′**.

The various forms of nicotinic acid can coordinate to copper(II) either through their endocyclic N-donor atom or through their carboxylato O-donor atoms to form a series of [Cu(dien)(nic)] complexes. The equilibrium geometries of the complexes computed at the B3LYP/6-31G(d,p) level are given in Figure 8 along with selected structural parameters.

All complexes adopt a distorted square-planar geometry. In [Cu(dien)(A′)] (**1A′**) the plane of **A′**, which is coordinated to Cu^{II} through its N-donor atom, is twisted almost 60° out of the coordination plane (Figure 8a). The same also holds true for the complex [Cu(dien)(C)] (**1C**), with **C** coordinated to copper(II) through its N-donor atom (Figure 8c). On the other hand, the torsion angle between the two planes is estimated to be diminished to around 25° in [Cu(dien)(B)] (**1B**) and [Cu(dien)(C′)] (**1C′**; Figures 8b and 8d, respectively), where ligands **B** and **C′** are coordinated to copper(II) through their carboxylato O-donor atoms. The three Cu–N coordination bonds formed between Cu^{II} and the dien ligand are longer in **1B** than in **1A**, **1C**, and **1C′**. The length of the Cu–N coordination bond formed between nicotinic acid and Cu^{II} decreases slightly upon going from

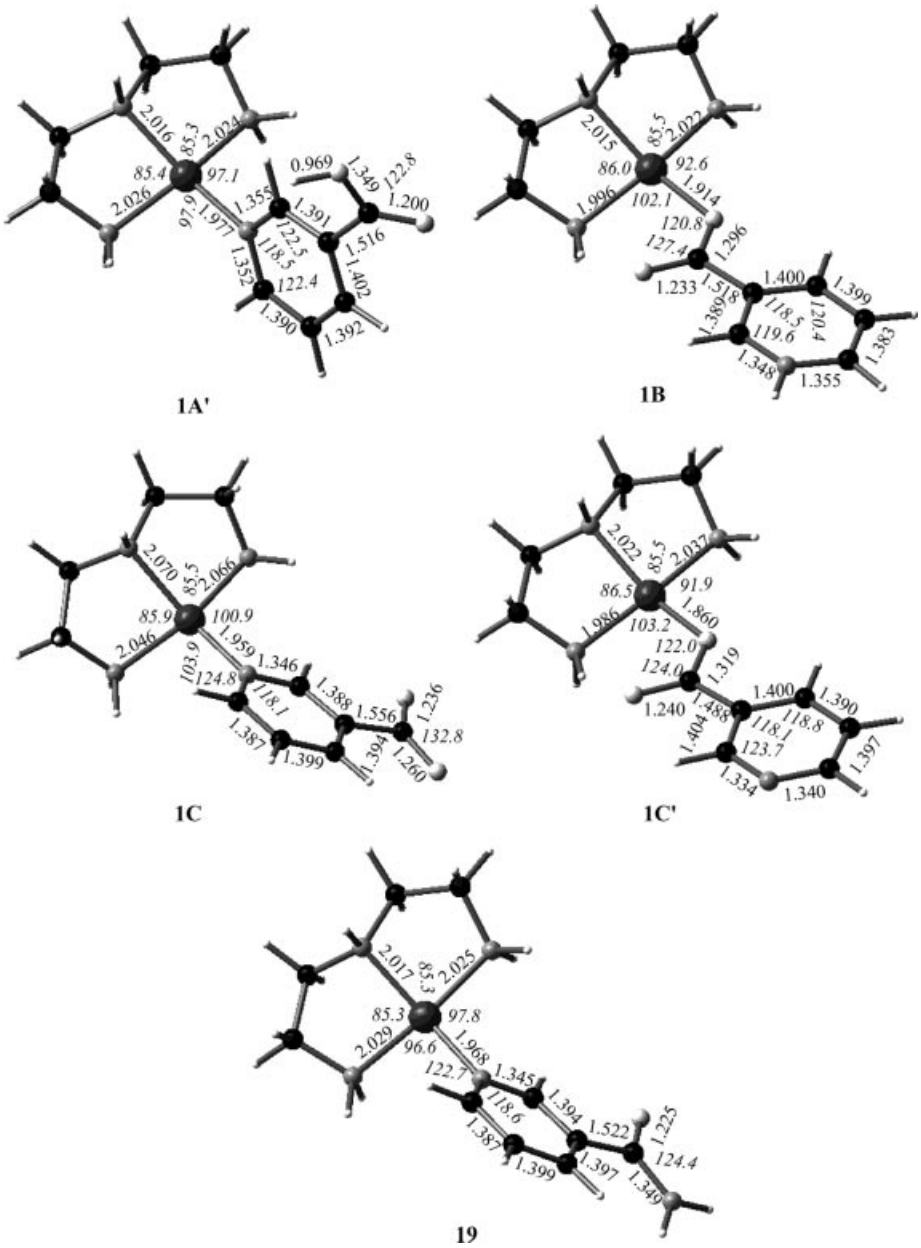

Figure 8. Equilibrium geometries of the [Cu(dien)(nic)] and [Cu(dien)(nica)] complexes computed at the B3LYP/6-31G(d,p) level of theory.

1A to **1B**. No significant changes in the structural parameters of the various nicotinic acid species could be observed upon coordination to Cu^{II}.

Selected energetic and electronic properties of the [Cu(dien)(nic)] and [Cu(dien)(nica)] complexes computed at the B3LYP/6-31G(d,p) level of theory are summarized in Table 3.

According to the natural bond orbital (NBO) analysis the Cu^{II} center acquires a positive natural charge of about 1.20–1.38 |e|. Based upon the natural electron configurations, the electron density is transferred from the N-donor atoms of the dien and nicotinic acid ligands to the 4s- and 3d-AOs of Cu^{II} (Table 2). Note that the natural electron configuration on the Cu^{II} central atom does not vary significantly upon going from **1A′** to **1C**. Interestingly, there is an increase in natural atomic charges of the N-donor atom of the nicotinic acid ligand in **1A′** and **1C** upon coordination to the Cu^{II} center, which could be attributed to a π-backbonding interaction between the 3d lone pair AOs of the Cu^{II} center and the vacant LUMO of **A′** or **C** (Figure 5). On the other hand, the same also holds true for **1B**, where an increase of the natural atomic charge on the O-donor atom of the nicotinic acid ligand is observed upon coordination. In all [Cu(dien)(nic)] complexes the spin density is mainly localized on the Cu^{II} and the N-donor atoms of the dien and nicotinic acid ligands, while in **1C** it is delocalized over the nicotinic acid ring and mainly on one of the carboxylate O donor atoms (Figure 8).

The equilibrium geometry of [Cu(dien)(nica)] (**18**), computed at the B3LYP/6-31G(d,p) level, is also given in Figure 8. The complex adopts a distorted square-planar geometry with the nicotinamide ligand being twisted almost 60° out of the coordination plane. The calculated structural parameters of **18** are in line with those obtained from the X-ray structural analysis for $[Cu(dien)(nica)(NO_3)_2]$ (**4**). No significant structural changes in nicotinamide could be observed upon coordination to Cu^{II}.

According to the NBO analysis the Cu^{II} center acquires a positive natural atomic charge of about 1.37 |e|. The natural electron configurations illustrate that the electron density is transferred from the N-donor atoms of the dien and nicotinamide ligands to the 4s- and 3d-AOs of Cu^{II} (Table 3). Also, there is an increase in the natural atomic charge of the N-donor atom upon coordination of the nicotinamide ligand to the Cu^{II} center in **18**, which could be attributed to a π-backbonding interaction between the 3d lone pair AOs of Cu^{II} and the LUMO of the nica ligand (Figure 7). Finally, the bond dissociation energy (BDE) of the nica ligand is predicted to be 67.2 kcal mol^{-1} at the B3LYP/6-31G(d,p) level.

Table 3. Selected energetic and electronic properties of the [Cu(dien)(nic)] and [Cu(dien)(nica)] complexes computed at the B3LYP/6-31G(d,p) level of theory.

Property	**1A′**	**1B**	**1C**	**1C′**	**18**
E [hartrees][a]	–2400.92235	–2400.98113	–2400.60805	–2400.68319	–2381.07330
BDE(Cu–X)[b]	54.2	116.6	265.7	312.8	67.2
Q(Cu)	1.38	1.39	1.20	1.35	1.37
Q(N1)[c]	–0.63	–0.48	–0.63	–0.45	–0.63
Q(O1)[d]	–0.49	–0.83	–0.5	–0.85	–0.59
Q(O2)	–0.68	–0.66	–0.66	–0.68	
Q(N2)[e]	–1.00	–1.01	–1.00	–1.01	–1.00
Q(N3)[e]	–1.00	–1.00	–1.00	–0.99	–1.00
Q(N4)[f]	–0.80	–0.80	–0.81	–0.79	–0.79
SD(Cu)[g]	0.65	0.68	0.44	0.68	0.65
SD(N1)	0.08	0.00	0.06	0.00	0.07
SD(O1)	0.00	0.07	0.01	0.10	0.01
SD(O2)	0.00	0.00	0.36	0.00	
SD(N2)	0.08	0.07	0.03	0.08	0.08
SD(N3)	0.09	0.08	0.04	0.07	0.09
SD(N4)	0.10	0.10	0.03	0.06	0.10
nec(Cu)[h]	$4s^{0.42}3d^{9.18}$	$4s^{0.41}3d^{9.17}$	$4s^{0.38}3d^{9.36}$	$4s^{0.41}3d^{9.20}$	$4s^{0.42}3d^{9.19}$
nec(N)	$2s^{1.34}2p^{4.26}$	$2s^{1.25}2p^{4.21}$	$2s^{1.35}2p^{4.26}$	$2s^{1.38}2p^{4.39}$	$2s^{1.34}2p^{4.26}$
nec(O1)	$2s^{1.74}2p^{4.75}$	$2s^{1.72}2p^{5.10}$	$2s^{1.72}2p^{4.93}$	$2s^{1.73}2p^{5.11}$	$2s^{1.70}2p^{4.87}$
nec(O2)	$2s^{1.68}2p^{4.99}$	$2s^{1.71}2p^{4.93}$	$2s^{1.74}2p^{4.75}$	$2s^{1.70}2p^{4.96}$	
nec(N2)	$2s^{1.46}2p^{4.52}$	$2s^{1.45}2p^{4.54}$	$2s^{1.45}2p^{4.52}$	$2s^{1.44}2p^{4.55}$	$2s^{1.46}2p^{4.52}$
nec(N3)	$2s^{1.46}2p^{4.52}$	$2s^{1.45}2p^{4.52}$	$2s^{1.45}2p^{4.52}$	$2s^{1.45}2p^{4.52}$	$2s^{1.46}2p^{4.52}$
nec(N4)	$2s^{1.39}2p^{4.39}$	$2s^{1.38}2p^{4.39}$	$2s^{1.38}2p^{4.40}$	$2s^{1.38}2p^{4.39}$	$2s^{1.39}2p^{4.38}$
bop(Cu–X)[i]	0.18	0.19	0.21	0.21	0.19
bop(Cu–N2)	0.16	0.16	0.14	0.16	0.16
bop(Cu–N3)	0.16	0.16	0.14	0.15	0.16
bop(Cu–N4)	0.16	0.15	0.14	0.14	0.16

[a] Total electronic energy plus zero point energy. [b] BDE is the bond dissociation energy [kcal mol^{-1}] for the Cu–X (X = N or O) bond between Cu^{II} and the X donor atom of nicotinic acid. [c] N1 donor atom of the nicotinic acid or nicotinamide ligands. [d] O1 donor atom of the nicotinic acid ligand. [e] N2 and N3 are the N-donor atoms of the dien ligand *cis* to nicotinic acid or nicotinamide. [f] N4 is the N-donor atom of the dien ligand *trans* to nicotinic acid or nicotinamide. [g] Spin density. [h] Natural electron configuration. [i] Mulliken bond overlap population.

Vibrational and Electronic Spectra of [Cu(dien)(nic)] and [Cu(dien)(nica)] Complexes

The unscaled vibrational frequencies in the vibrational spectra of the [Cu(dien)(nic)] and [Cu(dien)(nica)] complexes, calculated at the B3LYP/6-31G(d,p) level, appear within the range 3450–3530 cm^{-1}. The ν(C=O) stretching vibration for **A′**, **B**, and **C** appears at 1855, 1796, and 1591 cm^{-1} respectively. Upon coordination to Cu^{II} this vibration is red-shifted for **1A′**, **1C**, and **1C′**, appearing at 1876, 1688, and 1681 cm^{-1} respectively, while it is blue-shifted for **1B**, appearing at 1731 cm^{-1}. The N-coordination of nicotinic acid species is reflected in the calculated unscaled in-plane pyridinic ring deformation, δ_{py}, which is red-shifted in **1A′** and **1C** relative to the corresponding uncoordinated nicotinic acid species **A′** and **C**, appearing at 673 and 668 cm^{-1}, respectively. In contrast, it remains almost unaffected in **1B** and **1C′**, appearing at 635 and 633 cm^{-1} respectively. Moreover, the N-coordination of the nicotinamide is also reflected in the calculated in-plane pyridinic

Table 4. Principal electronic transitions, wavelengths (λ), and oscillator strengths (*f*) for [Cu(dien)(nic)] (**1B**) and [Cu(dien)(nica)] (**18**) computed at the B3LYP/6-31G(d,p) level.

	λ [nm]	*f*	Excitation	Composition of the participating MOs
1B				
	608 (618)[a]	0.001	HOMO–2 → SOMO	$(p_zO_{nic}) \rightarrow (d_\sigma Cu+2pN_{dien}+3pO_{nic})$
	270 (263)	0.128	HOMO–3 → SOMO	$(\pi^*_{nic}) \rightarrow (d_\sigma Cu+2pN_{dien}+3pO_{nic})$
			HOMO–10 → SOMO	$(d_\sigma Cu+2pN_{dien}) \rightarrow (d_\sigma Cu+2pN_{dien}+3pO_{nic})$
	248 (255)	0.034	HOMO–5 → SOMO	$(d_\pi Cu+2pN_{dien}+3pO_{nic}) \rightarrow (d_\sigma Cu+2pN_{dien}+3pO_{nic})$
	208	0.065	HOMO–4 → LUMO+1	$(d_\pi Cu+2pN_{dien}+3pO_{nic}) \rightarrow (\pi^*_{nic})$
	185	0.018	HOMO–6 → LUMO+1	$(d_\pi Cu+2pN_{dien}) \rightarrow (\pi^*_{nic})$
			HOMO–7 → LUMO+1	$(\pi^*_{nic}) \rightarrow (\pi^*_{nic})$
18				
	604 (612)[b]	0.005	HOMO–1 → SOMO	$(3pO_{nica}) \rightarrow (3pO_{nica})$
	533	0.002	HOMO–2 → SOMO	$(d_\sigma Cu+2pN_{dien}+\pi^*_{nica}) \rightarrow (3pO_{nica})$
	344	0.004	SOMO → LUMO	$(3pO_{nica}) \rightarrow (\pi^*_{nica})$
			HOMO–1 → LUMO	$(3pO_{nica}) \rightarrow (\pi^*_{nica})$
	272 (269)	0.14	HOMO–5 → SOMO	$(dCu+2pN_{dien}+\pi^*_{nica}) \rightarrow (3pO_{nica})$
	204	0.043	HOMO–15 → SOMO	$(dCu+2pN_{dien}) \rightarrow (3pO_{nica})$
	195	0.023	HOMO–16 → SOMO	$(\pi^*_{nica}) \rightarrow (3pO_{nica})$

[a] Experimental values for complex **5**. [b] Experimental values for complex **4**.

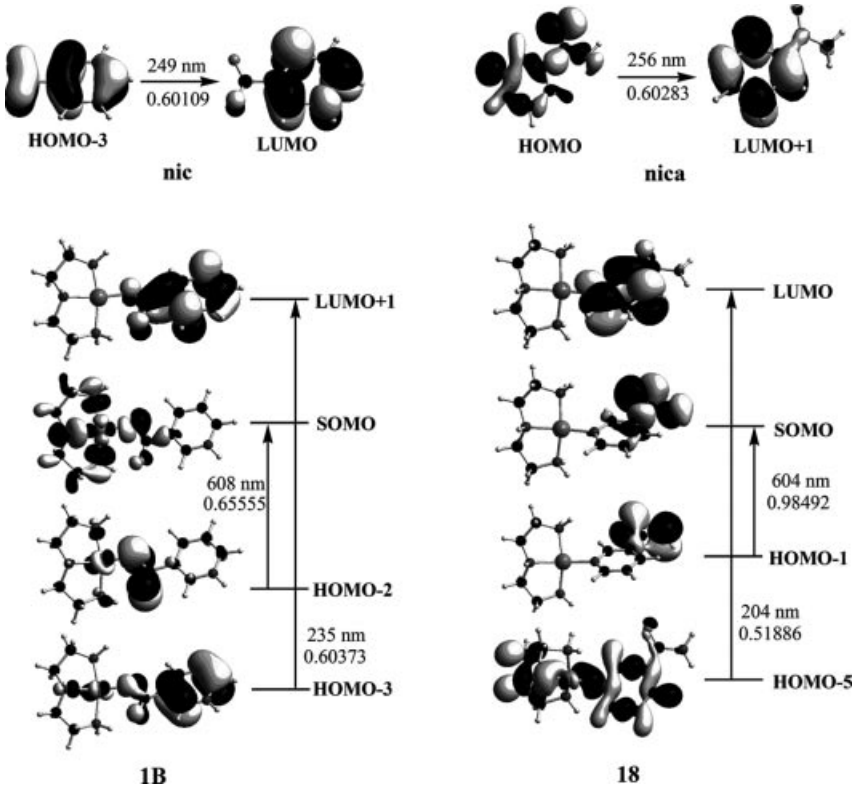

Figure 9. Single-electron transitions with the CI coefficients in the TD-DFT calculations for nic, nica, **1B**, and **18**.

ring deformation, δ_{py}, vibrational frequency, which in **18** appears at 801 and 672 cm^{-1}, while in uncoordinated nicotinamide it appears at 782 and 642 cm^{-1}, respectively.

TD-DFT calculations at the B3LYP/6-31G(d,p) level were performed in order to evaluate the properties of the excited states of [Cu(dien)(nic)] and [Cu(dien)(nica)] complexes. The principal singlet–singlet electronic transitions, excitation energies, and oscillator strengths, along with assignments, for **1B** and **18** are compiled in Table 4.

The computed electronic transitions for **1B** and **18** at 608 and 604 nm, respectively, are in excellent agreement with the experimental values. This broad and very intense band for 1B arises from the HOMO–2 → SOMO electronic transition (Figure 9). However, because of the highly delocalized MOs involved and the high mixing of the excited configurations due to the low symmetry of the complexes, it could not be assigned to one of the well-known LL, MLCT, LMCT, or d → d transitions. On the other hand, for **18** this band arises from a HOMO–1 → SOMO (Figure 9) electronic transition and can be classified as an intraligand (LL) transition.

The calculated electronic transitions at 249 and 256 nm for nic and nica, respectively, are in excellent agreement with the experimental values. These bands arise from π → π* and σ → π* type transitions for nic and nica, respectively (Figure 9). Upon coordination of the latter to Cu^{II} these bands are blue-shifted, appearing at 235 and 204 nm for **1B** and **18**, respectively.

Conclusions

We have reported the synthesis, structural characterization, and DFT study of the novel mixed-ligand Cu^{II} complexes formed upon reaction of [Cu(dien)X_2] (dien = diethylenetriamine; X = Br^-, NO_3^-) with pyridine (py), nicotinamide (nica), nicotinic acid (nic), and nicotinate anion (nic^-) in a 1:1 molar ratio. The salient structural features of the new complexes were determined by spectroscopic measurements (infrared and electronic spectra), while details of the structures were obtained by an X-ray structural investigation of the [Cu(dien)(nica)$(NO_3)_2$] complex. Conductivity measurements revealed the electrolytic nature of the complexes, while magnetic measurements are compatible with the d^9 electron configuration of the Cu^{II} centers. Moreover, DFT/B3LYP calculations of the structural, bonding, and electronic properties of the complexes corroborate the experimental evidence for the coordination of nicotinic acid preferably through the pyridine N-donor atom. Finally, the chemical reactivity of the Cu^{II} complexes towards a variety nucleophiles has been studied experimentally and discussed in relation with the electronic structure of the complexes computed at the DFT level.

Experimental Section

Materials and Instrumentation: All chemicals were purchased from Aldrich, EDH Chemicals and Merck, as reagent grade, and were used as received. C, H, and N were analyzed with a Perkin–Elmer 240B elemental analyser. IR spectra were recorded with a Perkin–Elmer Spectrum One spectrophotometer in the 400–4000 cm^{-1} region using KBr pellets and in the 200–400 cm^{-1} region using polyethylene disks. Electronic spectra were recorded with a Hitachi U-2001 spectrophotometer in the 200–1100 nm region, using 10-mm Teflon-stoppered quartz cells. Molar conductivities were measured with a WTW conductivity bridge and a calibrated dip-type cell. Magnetic susceptibilities on powdered samples were measured at room temperature using a Johnson–Matthey balance. Diamagnetic corrections were estimated from Pascal constants. The TG/DTA curves were obtained in a dynamic nitrogen atmosphere with a Setaram SETSYS-1200 thermal analyzer at a heating rate of 5 °C min^{-1} in a platinum crucible, in the temperature range 40–950 °C, with a sample mass of about 10 mg.

Synthesis of the Complexes: The starting material [Cu(dien)-$(NO_3)_2$] (**1**) was prepared according to a literature procedure,[9] while [Cu(dien)Br_2] (**2**) was prepared by the direct reaction of dien and $CuBr_2$.

[Cu(dien)(py)$(NO_3)_2$] (3): Pyridine (0.16 mL) was added dropwise to a suspension of**1** (0.581 g,2 mmol) in of methanol (20 mL). After stirring for 4 h, the solution was filtered to remove any impurities. Diethyl ether (10 mL) was then added to the filtrate, which was left at low temperature (5 °C) overnight. The dark-blue solid formed was isolated by filtration, washed with diethyl ether, and dried in air. Yield: 0.144 g (19%). $C_9H_{18}CuN_6O_6$ (369.82): calcd. C 29.23, H 4.91, N 22.72; found C 29.11, H 4.89, N 22.63. IR (KBr disk): ν_a(N–H) 3266 vs, ν_s(N–H) 3238 vs, ν_{sec}(N–H) 3196 vs, ν(C=N) 1608 s, ν(Cu–N) 523 m, ν(Cu–O) 456 m cm^{-1}. UV/Vis (H_2O): λ (log ε) = 616 nm (1.91), 263 sh, 256 sh, 249 (3.73), 243 sh. $\Lambda\mu$ (H_2O) = 247 μS cm^{-1}. μ_{eff} = 1.93 BM. M.p. 247 °C (dec.).

[Cu(dien)(nica)$(NO_3)_2$] (4): Complex **1** (1.456 g, 5 mmol) was dissolved in H_2O (2 mL) and further diluted with MeOH (10 mL). Nicotinamide (0.623 g, 5 mmol) in MeOH (15 mL) was added to this solution, with a concomitant darkening of the color. After the addition of diethyl ether (10 mL), the solution was left at low temperature (5 °C). After 14 h at this temperature, the dark-blue crystals formed were isolated by filtration, washed with diethyl ether, and dried at room temperature. Yield: 1.89 g (92%). $C_{10}H_{19}CuN_7O_7$ (412.85): calcd. C 29.09, H 4.64, N 23.75; found C 29.06, H 4.56, N 23.68. IR (KBr disk): ν_a(N–H) 3273 vs, ν_s(N–H) 3244 s, ν_{sec}(N–H) 3156 s-br, ν(C=O) 1693 vs, ν(C=N) 1603 s, ν(Cu–N) 537 m, ν(Cu–O) 461 m cm^{-1}. UV/Vis (H_2O): λ (log ε) = 612 nm (1.87), 269 sh, 254 (3.72). $\Lambda\mu$ (H_2O) = 206 μS cm^{-1}. μ_{eff} = 1.82 BM. M.p. 193–195 °C.

[Cu(dien)(nic^-)$(NO_3)(H_2O)$]·H_2O (5): A solution of nicotinic acid (0.62 g,5 mmol) in methanol (10 mL) was added to an aqueous solution of NaOH (0.2 g in 2 mL) with vigorous stirring. This solution of sodium nicotinate was added to a solution of **1** (1.45 g, 5 mmol) in H_2O/MeOH (1 mL/10 mL). The final solution was left overnight at room temperature. The blue needles formed were isolated by filtration, washed with diethyl ether, and dried at room temperature. Yield: 0.81 g (42%). $C_{10}H_{21}CuN_5O_7$ (386.85): calcd. C 31.05, H 5.47, N 18.10; found C 31.02, H 5.43, N 18.02. IR (KBr disk): ν_a(N–H) 3270 vs, ν_s(N–H) 3204 vs, ν_{sec}(N–H) 3163 vs, ν(C=O) 1668 s, ν(C=N) 1591 vs, ν(Cu–N) 527 s, ν(Cu–O) 449 m cm^{-1}. UV/Vis (H_2O): λ (log ε) = 618 nm (1.62), 269 sh, 262 sh, 255(3.84). $\Lambda\mu$ (H_2O) = 164 μS cm^{-1}. μ_{eff} = 1.76 BM. M.p. 141 °C (dec.).

[Cu(dien)(nic^-)(Br)(H_2O)]·$2H_2O$ (6): A solution of nicotinic acid (0.262 g, 2.5 mmol) in methanol (10 mL) was added to an aqueous solution of NaOH (0.2 g in 2 mL) with vigorous stirring. This solu-

tion of sodium nicotinate was added to a solution of **2** (0.82 g, 2.5 mmol) in H_2O/MeOH (2 mL/10 mL). The final solution was stirred to give a blue solid, which was isolated by filtration, washed with diethyl ether, and dried at room temperature. Yield: 0.44 g (40%). $C_{10}H_{23}BrCuN_4O_5$ (422.76): calcd. C 28.41, H 5.48, N 13.25; found C 28.48, H 5.49, N 13.28. IR (KBr disk): ν_a(N–H) 3271 s, ν_s(N–H) 3203 s, ν_{sec}(N–H) 3163 m, ν(C=O) 1667 m, ν(C=N) 1591 s, ν(Cu–N) 525 m, ν(Cu–O) 448 m cm^{-1}. UV/Vis (H_2O): λ ($\log\varepsilon$) = 608 (1.93), 269 sh, 262 sh, 255 (3.77), 214 sh. $\Lambda\mu$ (H_2O) = 173 $\mu S\,cm^{-1}$. μ_{eff} = 1.80 BM. M.p. 131–133 °C.

[Cu(dien)(NO_3)(nic$^-$)(N^7-Guo)]·5H_2O (7): A solution of sodium nicotinate (5 mmol) in H_2O/EtOH (1 mL/10 mL) was added dropwise to a water/methanol (1 mL/10 mL) solution of **1** (1.453 g, 5 mmol) and the mixture stirred continuously for 5 min. After the addition of guanosine (Guo) (1.516 g, 5 mmol) in small quantities and ethanol (80 mL), the new suspension was further stirred for 12 h so as to allow complete reaction of Guo, after which the blue-purple solid formed was isolated by filtration, washed with diethyl ether, and dried at room temperature. Yield: 3.55 g (98%). $C_{20}H_{40}CuN_{10}O_{15}$ (724.14): calcd. C 33.17, H 5.57, N 19.34; found C 33.52, H 5.66, N 19.71. IR (KBr disk): ν_a(N–H) 3270 vs,br, ν_s(N–H) 3226 vs-br, ν_{sec}(N–H) 3165 vs, ν(C=O) 1680 s, ν(C=N)1591 s, ν(Cu–N) 527 m, ν(Cu–O) 449 w cm^{-1}. UV/Vis (H_2O): λ ($\log\varepsilon$) = 612 (1.86), 269 sh, 253 (4.24). $\Lambda\mu$ (H_2O) = 159 $\mu S\,cm^{-1}$. μ_{eff} = 1.83 BM. M.p. 108–110 °C.

Table 5. Crystal data, data collection and refinement details for [Cu(dien)(nica)(NO_3)$_2$] (**4**).

Empirical formula	$C_{10}H_{19}CuN_7O_7$
Formula mass	412.86
Crystal size [mm]	0.45×0.15×0.10
Crystal system	monoclinic
Space group	$P2_1/c$
a [Å]	8.1636(14)
b [Å]	15.7067(18)
c [Å]	12.7266(13)
β [°]	98.451(12)
Cell volume [Å^3]	1614.1(4)
Z	4
T [K]	293(2)
$D_{calcd.}$ [$Mg\,m^{-3}$]	1.699
μ [mm^{-1}]	1.405
F(000)	852
Diffractometer	upgraded Philips PW1100
Radiation	Mo-K_α (0.71073 Å)
Monochromator	graphite
Data-collection method	$\theta/2\theta$
2θ range [°]	4.14–52.04
Index ranges	$-10 \le h \le 9$
	$-19 \le k \le 19$
	$0 \le l \le 15$
Reflections collected	6710
Independent reflections (R_{int})	3167 (0.0737)
Observed reflections [$I > 2\sigma(I)$]	1993
Completeness to θ = 26.02°	99.9 (%)
Max./min. transmission factors	0.870, 0.498
Refinement method	full-matrix least squares
Data/restraints/parameters	3167/0/283
Final R indices [$I > 2\sigma(I)$][a]	R_1 = 0.0403, wR_2 = 0.0799
R indices (all data)	R_1 = 0.0970, wR_2 = 0.0949
GOF	0.982
Maximum shift/error	0.007
ρ_{max}, ρ_{min} [e Å^{-3}]	0.510, –0.408

[a] R indices and GOF defined as: $R_1 = \Sigma||F_o| - |F_c||/\Sigma|F_o|$, $wR_2 = [\Sigma w(F_o^2 - F_c^2)^2/\Sigma w(F_o^2)^2]^{1/2}$, GOF = $\{\Sigma\,[w(F_o^2 - F_c^2)^2]/(n - p)\}^{1/2}$, n = no. of reflections, p = no. of parameters refined.

Computational Details: The structural, electronic, and energetic properties of all compounds were computed with Becke's three-parameter hybrid functional[33] combined with the Lee–Yang–Parr correlation functional,[34] abbreviated as B3LYP, using the 6-31G(d,p) basis set. In all computations no constraints were imposed on the geometry. Full geometry optimization was performed for each structure using Schlegel's analytical gradient method[35] and the attainment of the energy minimum was verified by calculating the vibrational frequencies that result in absence of imaginary eigenvalues. All calculations were performed using the GAUSSIAN03 suite of programs.[36]

X-ray Crystallographic Study: Crystal data, data collection, and refinement details for [Cu(dien)(nica)(NO_3)$_2$] are given in Table 5. Cell parameters were calculated by least-squares refinement of the setting angles of 21 reflections and their equivalents ($13.60° < 2\theta < 22.20°$). Intensities were collected using graphite-monochromated Mo-K_α radiation and a scintillation counter.[37] Three standard reflections monitored every 120 min showed no significant deterioration. They were used to scale the intensities, which were further corrected for Lorentz and polarization effects,[38] as well as for absorption (empirical ψ-scan method).[39] Most calculations were performed with the WinGX system of programs.[40] The structure was solved by direct methods and subsequent difference Fourier syntheses with the SHELXS-97 program[41] and refined with the SHELXL-97 program.[42] Some of the geometrical calculations were performed with the PLATON program.[43] All the non-hydrogen atoms were refined anisotropically. The hydrogen atoms could be located on the difference Fourier map, and in the final refinement step their positions were varied freely but their displacement parameters were constrained to 1.2 U_{eq} of the corresponding values of the atoms to which they are bonded. CCDC-264390 contains the supplementary crystallographic data for this paper. These data can be obtained free of charge from The Cambridge Crystallographic Data Center via www.ccdc.cam.ac.uk/data_request/cif.

Acknowledgments

The financial support of this work by the Greek General Secretariat for Research and Technology and the European Commission within the frame of the PENED01 projects is gratefully acknowledged (grant no. 01EΔ367).

[1] Y. Miwa, T. Mizuno, K. Tsuchida, T. Taga, Y. Iwata, *Acta Crystallogr., Sect. B* **1999**, *55*, 78–84.
[2] C. B. Aakeröy, A. M. Beatty, *Chem. Commun.* **1998**, 1067.
[3] J. Yarks, L. He, J. D. Adams Jr, *Pharmacol. Biochem. Behav.* **2004**, *78*, 179–183.
[4] M. M. Mycek, R. A. Harvey, P. C. Champe, *Pharmacology*, 2nd ed., Lippincott-Raven, Philadelphia, **1997**.
[5] P. Zachariadis, S. Hadjikakou, N. Hadjiliadis, A. Michaelides, S. Skoulika, Y. Ming, Y. Xiaolin, *Inorg. Chim. Acta* **2003**, *343*, 361–365.
[6] Z. Chohan, A. Rauf, S. Noreen, A. Scozzafava, C. Supuran, *J. Enzyme Inhib. Med. Chem.* **2002**, *17*, 101–106.
[7] S. Osinsky, I. Levitin, L. Campanella, P. Wadman, *Exp. Oncol.* **2004**, *26*, 140–144.
[8] M. Palicová, P. Segl'a, D. Mikloš, M. Kopcová, M. Melník, B. Dudová, D. Hudecová, T. Glowiak, *Polyhedron* **2000**, *19*, 2689–2695.
[9] R. Allman, M. Krestl, C. Bolos, G. Manoussakis, G. St. Nikolov, *Inorg. Chim. Acta* **1990**, *175*, 255–260.
[10] E. Şahin, S. İde, A. Ataç, Ş. Yurdakul, *J. Mol. Struct.* **2002**, *616*, 253–258.

[11] K. Nakamoto, *Infrared and Raman Spectra of Inorganic and Coordination Compounds*, 4th ed., John Wiley & Sons, Inc., New York, **1992**, pp. 256, 324.
[12] S. Bayari, A. Ataç, Ş. Yurdakul, *J. Mol. Struct.* **2003**, *655*, 163–170.
[13] S. Çakir, İ. Bulut, P. Naumov, E. Biçer, O. Çakir, *J. Mol. Struct.* **2001**, *560*, 1–7.
[14] E. A. Velcheva, L. I. Daskalova, *J. Mol. Struct.* **2005**, *741*, 85–92.
[15] P. Koczoń, J. Cz. Dobrowolski, W. Lewandowski, A. P. Mazurek, *J. Mol. Struct.* **2003**, *655*, 89–95.
[16] S. İde, A. Ataç, Ş. Yurdakul, *J. Mol. Struct.* **2002**, *605*, 103–107.
[17] A. B. P. Lever, *Inorganic Electronic Spectroscopy*, 2nd ed., Elsevier, Amsterdam, **1984**.
[18] W. J. Geary, *Coord. Chem. Rev.* **1971**, *7*, 81–122.
[19] C.-W. Yeh, M.-C. Suen, H.-L. Hu, J.-D. Chen, J.-C.- Wang, *Polyhedron* **2004**, *23*, 1947–1952.
[20] G. Bergerhoff, *DIAMOND, Visual Crystal Structure Information System*, Gerhard-Domagk-Str. 1, 53121 Bonn, Germany, **1996**.
[21] C. A. Bolos, P. C. Christidis, S. T. Triantafyllou, *Polyhedron* **1998**, *17*, 2719–2726.
[22] F.-M. Nje, Z.-M. Wang, Y.-M. Li, Y.-F. Zhao, C.-H. Yan, *Acta Crystallogr., Sect. C* **1998**, *54*, 1853–1855.
[23] Y. Zhang, P. Zhang, J. Li, M. Nishiura, *J. Mol. Struct.* **2001**, *570*, 37–42.
[24] M. Sato, S. Nagae, K. Ohmae, J. Nakaya, K. Miki, N. Kasai, *J. Chem. Soc., Dalton Trans.* **1986**, 1949–1953.
[25] Q. Lu, A. Singh, J. R. Deschamps, E. L. Chang, *Inorg. Chim. Acta* **2000**, *309*, 82–90.
[26] G. R. Hall, D. M. Duggan, D. N. Hendrickson, *Inorg. Chem.* **1975**, *14*, 1956–1964.
[27] A. Nielsen, A. D. Bond, C. J. McKenzie, *Acta Crystallogr., Sect. E* **2005**, *61*, m478–m480.
[28] M. K. Urtiaga, M. I. Arriortua, R. Cortes, T. Rojo, *Acta Crystallogr., Sect. C* **1996**, *52*, 3007–3009.
[29] C. A. Bolos, P. C. Christidis, S. T. Triantafyllou, *Polyhedron* **1998**, *17*, 2719–2726.
[30] H.-M. Hu, H. S.-Sun, X.-H. Chen, Q. Zhao, Y. Pan, X.-Y. Huang, X.-Z. You, *Acta Crystallogr., Sect. C* **1997**, *53*, 276–278.
[31] R. W. Green, H. K. Tong, *J. Am. Chem. Soc.* **1956**, *78*, 4896.
[32] O. Sala, N. S. Gonçalves, L. K. Noda, *J. Mol. Struct.* **2001**, *565–566*, 411–416.
[33] a) A. D. Becke, *J. Chem. Phys.* **1992**, *96*, 2155; b) A. D. Becke, *J. Chem. Phys.* **1993**, *98*, 5648.
[34] C. Lee, W. Yang, R. G. Parr, *Phys. Rev. B* **1988**, *37*, 785.
[35] H. B. Schlegel, *J. Comput. Chem.* **1982**, *3*, 214.
[36] M. J. Frisch, G. W. Trucks, H. B. Schlegel, G. E. Scusseria, M. A. Robb, J. R. Cheeseman, V. G. Zakrzewski, J. A. Montgomery, T. Vreven, K. N. Kudin, J. C. Burant, J. M. Millan, S. S. Iyengar, J. Tomasi, V. Barone, B. Mennucci, M. Cossi, G. Scalmani, N. Rega, G. A. Petersson, H. Nakatsuji, M. Hada, M. Ehara, K. Toyota, F. R., J. Hasegawa, M. Ishida, T. Nakajima, Y. Honda, O. Kitao, H. Nakai, M. Klene, X. Li, J. E. Knox, H. P. Hratchian, J. B. Cross, C. Adamo, J. Jaramillo, R. Gomperts, R. E. Stratmann, O. Yazyev, A. J. Austin, R. Cammi, C. Pomelli, J. W. Ochterski, P. Y. Ayala, K. Morokuma, G. A. Voth, P. Salvador, J. J. Dannenberg, V. G. Zakrzewski, S. Dapprich, A. D. Daniels, M. C. Strain, O. Farkas, D. K. Malick, A. D. Rabuck, K. Raghavachari, J. B. Foresman, J. V. Ortiz, Q. Cui, A. G. Baboul, S. Clifford, J. Cioslowski, B. B. Stefanov, G. Liu, A. Liashenko, P. Piskorz, I. Komaromi, R. L. Martin, D. J. Fox, T. Keith, M. A. Al-Laham, C. Y. Peng, A. Nanayakkara, M. Challacombe, P. M. W. Gill, B. Johnson, W. Chen, M. W. Wong, C. Gonzalez, J. A. Pople, *Gaussian 03, Revision B.02*, Gaussian, Inc., Pittsburgh PA, USA, **200**3.
[37] Stoe & Cie, *DIF4 Diffractometer Control Program*, version 6.2, Stoe & Cie, Darmstadt, Germany, **1988**.
[38] Stoe & Cie, *REDU4, Data Reduction Program*, version 6.2, Stoe & Cie, Darmstadt, Germany, **1988**.
[39] Stoe & Cie, *EMPIR, Data Setup for Empirical Absorption Correction*, version 6.2, Stoe & Cie, Darmstadt, Germany, **1988**.
[40] "WinGX, An Integrated System of Windows Programs for the Solution, Refinement and Analysis of Single Crystal Diffraction Data", vers. 1.70.00: L. J. Farrugia, *J. Appl. Crystallogr.* **1999**, *32*, 837.
[41] G. M. Sheldrick, *SHELXS97, Program for Crystal Structure Solution*, University of Göttingen, Germany, **1997**.
[42] G. M. Sheldrick, *SHELXL97, Program for Crystal Structure Refinement*, University of Göttingen, Germany, **1997**.
[43] A. L. Spek, *J. Appl. Crystallogr.* **2003**, *36*, 7–13.

Received: October 7, 2005
Published Online: March 22, 2006

